

Measurement of the Λ_c^+ Lifetime

A. H. Mahmood,¹ S. E. Csorna,² I. Danko,² K. W. McLean,² Sz. Márka,² Z. Xu,² R. Godang,³ K. Kinoshita,^{3,*} I. C. Lai,³ S. Schrenk,³ G. Bonvicini,⁴ D. Cinabro,⁴ S. McGee,⁴ L. P. Perera,⁴ G. J. Zhou,⁴ E. Lipeles,⁵ S. P. Pappas,⁵ M. Schmidtler,⁵ A. Shapiro,⁵ W. M. Sun,⁵ A. J. Weinstein,⁵ F. Würthwein,^{5,†} D. E. Jaffe,⁶ G. Masek,⁶ H. P. Paar,⁶ E. M. Potter,⁶ S. Prell,⁶ V. Sharma,⁶ D. M. Asner,⁷ A. Eppich,⁷ T. S. Hill,⁷ R. J. Morrison,⁷ H. N. Nelson,⁷ R. A. Briere,⁸ G. P. Chen,⁸ B. H. Behrens,⁹ W. T. Ford,⁹ A. Gritsan,⁹ J. Roy,⁹ J. G. Smith,⁹ J. P. Alexander,¹⁰ R. Baker,¹⁰ C. Bebek,¹⁰ B. E. Berger,¹⁰ K. Berkelman,¹⁰ F. Blanc,¹⁰ V. Boisvert,¹⁰ D. G. Cassel,¹⁰ M. Dickson,¹⁰ P. S. Drell,¹⁰ K. M. Ecklund,¹⁰ R. Ehrlich,¹⁰ A. D. Foland,¹⁰ P. Gaidarev,¹⁰ R. S. Galik,¹⁰ L. Gibbons,¹⁰ B. Gittelman,¹⁰ S. W. Gray,¹⁰ D. L. Hartill,¹⁰ B. K. Heltsley,¹⁰ P. I. Hopman,¹⁰ C. D. Jones,¹⁰ J. Kandaswamy,¹⁰ D. L. Kreinick,¹⁰ M. Lohner,¹⁰ A. Magerkurth,¹⁰ T. O. Meyer,¹⁰ N. B. Mistry,¹⁰ E. Nordberg,¹⁰ J. R. Patterson,¹⁰ D. Peterson,¹⁰ D. Riley,¹⁰ J. G. Thayer,¹⁰ D. Uner,¹⁰ B. Valant-Spaight,¹⁰ A. Warburton,¹⁰ P. Avery,¹¹ C. Prescott,¹¹ A. I. Rubiera,¹¹ J. Yelton,¹¹ J. Zheng,¹¹ G. Brandenburg,¹² A. Ershov,¹² Y. S. Gao,¹² D. Y.-J. Kim,¹² R. Wilson,¹² T. E. Browder,¹³ Y. Li,¹³ J. L. Rodriguez,¹³ H. Yamamoto,¹³ T. Bergfeld,¹⁴ B. I. Eisenstein,¹⁴ J. Ernst,¹⁴ G. E. Gladding,¹⁴ G. D. Gollin,¹⁴ R. M. Hans,¹⁴ E. Johnson,¹⁴ I. Karliner,¹⁴ M. A. Marsh,¹⁴ M. Palmer,¹⁴ C. Plager,¹⁴ C. Sedlack,¹⁴ M. Selen,¹⁴ J. J. Thaler,¹⁴ J. Williams,¹⁴ K. W. Edwards,¹⁵ R. Janicek,¹⁶ P. M. Patel,¹⁶ A. J. Sadoff,¹⁷ R. Ammar,¹⁸ A. Bean,¹⁸ D. Besson,¹⁸ R. Davis,¹⁸ N. Kwak,¹⁸ X. Zhao,¹⁸ S. Anderson,¹⁹ V. V. Frolov,¹⁹ Y. Kubota,¹⁹ S. J. Lee,¹⁹ R. Mahapatra,¹⁹ J. J. O'Neill,¹⁹ R. Poling,¹⁹ T. Riehle,¹⁹ A. Smith,¹⁹ C. J. Stepaniak,¹⁹ J. Urheim,¹⁹ S. Ahmed,²⁰ M. S. Alam,²⁰ S. B. Athar,²⁰ L. Jian,²⁰ L. Ling,²⁰ M. Saleem,²⁰ S. Timm,²⁰ F. Wappler,²⁰ A. Anastassov,²¹ J. E. Duboscq,²¹ E. Eckhart,²¹ K. K. Gan,²¹ C. Gwon,²¹ T. Hart,²¹ K. Honscheid,²¹ D. Hufnagel,²¹ H. Kagan,²¹ R. Kass,²¹ T. K. Pedlar,²¹ H. Schwarthoff,²¹ J. B. Thayer,²¹ E. von Toerne,²¹ M. M. Zoeller,²¹ S. J. Richichi,²² H. Severini,²² P. Skubic,²² A. Undrus,²² S. Chen,²³ J. Fast,²³ J. W. Hinson,²³ J. Lee,²³ D. H. Miller,²³ E. I. Shibata,²³ I. P. J. Shipsey,²³ V. Pavlunin,²³ D. Cronin-Hennessy,²⁴ A. L. Lyon,²⁴ E. H. Thorndike,²⁴ C. P. Jessop,²⁵ H. Marsiske,²⁵ M. L. Perl,²⁵ V. Savinov,²⁵ X. Zhou,²⁵ T. E. Coan,²⁶ V. Fadeyev,²⁶ Y. Maravin,²⁶ I. Narsky,²⁶ R. Stroynowski,²⁶ J. Ye,²⁶ T. Wlodek,²⁶ M. Artuso,²⁷ R. Ayad,²⁷ C. Boulahouache,²⁷ K. Bukin,²⁷ E. Dambasuren,²⁷ S. Karamov,²⁷ G. Majumder,²⁷ G. C. Moneti,²⁷ R. Mountain,²⁷ S. Schuh,²⁷ T. Skwarnicki,²⁷ S. Stone,²⁷ G. Viehhauser,²⁷ J. C. Wang,²⁷ A. Wolf,²⁷ J. Wu,²⁷ and S. Kopp²⁸

(CLEO Collaboration)

¹University of Texas–Pan American, Edinburg, Texas 78539

²Vanderbilt University, Nashville, Tennessee 37235

³Virginia Polytechnic Institute and State University, Blacksburg, Virginia 24061

⁴Wayne State University, Detroit, Michigan 48202

⁵California Institute of Technology, Pasadena, California 91125

⁶University of California, San Diego, La Jolla, California 92093

⁷University of California, Santa Barbara, California 93106

⁸Carnegie Mellon University, Pittsburgh, Pennsylvania 15213

⁹University of Colorado, Boulder, Colorado 80309-0390

¹⁰Cornell University, Ithaca, New York 14853

¹¹University of Florida, Gainesville, Florida 32611

¹²Harvard University, Cambridge, Massachusetts 02138

¹³University of Hawaii at Manoa, Honolulu, Hawaii 96822

¹⁴University of Illinois, Urbana-Champaign, Illinois 61801

¹⁵Carleton University, Ottawa, Ontario, Canada K1S 5B6

and the Institute of Particle Physics, Canada

¹⁶McGill University, Montréal, Québec, Canada H3A 2T8

and the Institute of Particle Physics, Canada

¹⁷Ithaca College, Ithaca, New York 14850

¹⁸University of Kansas, Lawrence, Kansas 66045

¹⁹University of Minnesota, Minneapolis, Minnesota 55455

²⁰State University of New York at Albany, Albany, New York 12222

²¹Ohio State University, Columbus, Ohio 43210

²²University of Oklahoma, Norman, Oklahoma 73019

²³Purdue University, West Lafayette, Indiana 47907

²⁴University of Rochester, Rochester, New York 14627

²⁵Stanford Linear Accelerator Center, Stanford University, Stanford, California 94309

²⁶*Southern Methodist University, Dallas, Texas 75275*²⁷*Syracuse University, Syracuse, New York 13244*²⁸*University of Texas, Austin, Texas 78712*

(Received 15 November 2000)

The Λ_c^+ lifetime is measured using 9.0 fb^{-1} of e^+e^- annihilation data collected on or just below the $Y(4S)$ resonance with the CLEO II.V detector at CESR. Using an unbinned maximum likelihood fit, the Λ_c^+ lifetime is measured to be $179.6 \pm 6.9(\text{stat}) \pm 4.4(\text{syst}) \text{ fs}$. The precision of this colliding beam measurement is comparable to other measurements, which are based on fixed-target experiments, with different systematic uncertainties.

DOI: 10.1103/PhysRevLett.86.2232

PACS numbers: 14.20.Lq, 13.30.Eg

Lifetime measurements of heavy quark mesons and baryons provide an important window into the non-perturbative sector of heavy quark decay. Contrary to initial expectations [1], mechanisms other than spectator quark decay make significant contributions to the lifetimes of weakly decaying charm mesons and baryons. Charm baryon lifetimes differ by large amounts (e.g., $\tau_{\Xi_c^+}:\tau_{\Lambda_c^+}:\tau_{\Xi_c^0} \sim 4:2:1$) [2], as is also seen in the charm mesons. However, the underlying reasons for this pattern may be different than for the mesons as W exchange in baryon decay is neither helicity nor color suppressed. Other effects, such as Pauli interference, may also play a different role in the baryon sector [1]. This paper reports a new measurement of the lifetime of the Λ_c^+ , the lowest-mass charm baryon, with a precision comparable to that from measurements of the charm meson lifetimes. The data used in this analysis were obtained in an e^+e^- colliding beam environment, where the event topologies and backgrounds are very different from those encountered in high energy fixed-target experiments [3], which have historically provided the most precise measurements of charm hadron lifetimes [2].

This analysis uses an integrated luminosity of 9.0 fb^{-1} of e^+e^- annihilation data recorded with the CLEO II.V detector at the Cornell Electron Storage Ring (CESR). The data were taken at energies at or slightly below the $Y(4S)$ resonance ($\sqrt{s} = 10.58 \text{ GeV}$) and contain approximately $11 \times 10^6 e^+e^- \rightarrow c\bar{c}$ events. The CLEO II.V detector upgrade consists of a redesigned interaction region (IR) and a change in the gas used in the primary tracking volume (refer to [4] for a detector description before the upgrade). The IR consists of a small-radius, low-mass beam pipe surrounded by a three-layer double-sided silicon vertex detector (SVX). The SVX records precision three-dimensional tracking information close to the interaction point [5,6]. The proximity of the SVX to the IR, combined with the low mass beam-pipe, delivered excellent vertex resolution. The momentum resolution was enhanced as a result of changing the primary tracking volume gas from a 50:50 mixture of argon-ethane to a 60:40 mixture of helium-propane. This change increased the hit efficiency and decreased the effects of multiple scattering. The helium-propane replacement also enhanced specific ionization information used for particle identification. Further, to optimize the data from the upgraded detector, a Kalman filter track reconstruction package [7] was imple-

mented. The response of the CLEO detector to both signal and background events was simulated in detail using a GEANT-based [8] Monte Carlo package.

The Λ_c^+ is reconstructed in the $pK^-\pi^+$ decay mode (the charge conjugate mode is implied throughout this paper). General track quality and event shape cuts are used to remove poorly reconstructed tracks and nonhadronic events. A decay vertex measurement is needed for a proper time measurement, so we require at least two of the three decay tracks to have 2 or more SVX hits simultaneously on a track in both the xy and rz [9] views. The efficiency to have two or more SVX hits simultaneously in both views is 95% per track, yielding 99% efficiency per Λ_c^+ ; the average decay vertex resolution was about $110 \mu\text{m}$.

The combinatoric background to the Λ_c^+ signal is suppressed by taking advantage of the detector upgrades. Tracks forming a Λ_c^+ candidate are required to originate from a common vertex ($x_{\text{dec}}, y_{\text{dec}}, z_{\text{dec}}$) in a three-dimensional vertex fit. We require the vertex fit probability to be >0.001 . Particle identification information from specific ionization must be consistent with the Λ_c^+ daughter hypothesis. Electrons are rejected using drift chamber and calorimeter information. Backgrounds tend to populate the low track momentum spectrum and low Λ_c^+ momentum spectrum. Each decay track is therefore required to have momentum greater than $0.3 \text{ GeV}/c$. We remove Λ_c^+ 's from B mesons by requiring the Λ_c^+ momentum to be greater than $2.6 \text{ GeV}/c$. As a result of these cuts, the selected Λ_c^+ 's have an average momentum of $3.3 \text{ GeV}/c$.

Combinatoric backgrounds from random combinations of tracks from D^0 , D^+ , and D_s^+ decays, which may populate the reconstructed mass region nonuniformly and bias the lifetime result, are studied using data and Monte Carlo. From tests using CLEO data and Monte Carlo simulated events, we find that $D^+ \rightarrow K^-\pi^+\pi^+$ events (where one of the pions passes the proton requirements) preferentially populate the reconstructed mass region above the Λ_c^+ mass peak. Such events are a potentially problematic kinematic reflection that we remove by rejecting candidates whose reconstructed mass is consistent with a D^+ mass when the proton hypothesis is changed to a pion hypothesis. All other backgrounds (e.g., $D_s^+ \rightarrow \phi\pi^+$) are found to be either uniform throughout the mass region or small enough not to affect the final lifetime result.

The reconstructed mass distribution is fit using two Gaussians constrained to a common mean for the signal and a linear function for the background. The widths of the Gaussians are denoted as σ_{narrow} and σ_{broad} . The reconstructed mass distribution of the Λ_c^+ candidates is shown in Fig. 1, and a fit to the data yields $4749 \pm 124 \Lambda_c^+ \rightarrow pK^-\pi^+$ signal events, $\sigma_{\text{narrow}} = 3.6 \text{ MeV}/c^2$, and $\sigma_{\text{broad}} = 10.1 \text{ MeV}/c^2$. The $\chi^2/\text{d.o.f.}$ of the reconstructed mass fit is 181/163. The fraction of background in the mass region within $7 \text{ MeV}/c^2$ ($1.94 \sigma_{\text{narrow}}$) of the fitted Λ_c^+ mass value is 27.2%, while 85.2% of the Λ_c^+ 's are within this region as well.

The Λ_c^+ production point ($x_{\text{prod}}, y_{\text{prod}}, z_{\text{prod}}$) is needed for the proper time determination. A beam centroid determined for each CESR fill (approximately 1 h long) from two-track and hadronic events provides an estimate of the Λ_c^+ production point. The dimensions of the beam profile are about $350 \mu\text{m}$, $7 \mu\text{m}$, and 1 cm along the x , y , and z directions, respectively, as determined by CESR [10] optics. Given the extent of the profile in x and z , the measurement is effectively determined by the y component. The y components of the decay length, $l_y \equiv y_{\text{dec}} - y_{\text{prod}}$, and Λ_c^+ momentum, $p_{y\Lambda_c^+}$, are used to determine the proper decay times, calculated from $t = m_{\Lambda_c^+} l_y / c p_{y\Lambda_c^+}$ using the Particle Data Group (PDG) [2] world average for $m_{\Lambda_c^+}$. The decay length variance σ_l^2 is calculated using the results of the vertex fit and the beam profile dimension uncertainties. The proper time distribution for the Λ_c^+ candidates within $7 \text{ MeV}/c^2$ of the Λ_c^+ signal peak is shown in Fig. 2. The average decay length is about $80 \mu\text{m}$, comparable to the vertex resolution. Since all Λ_c^+ candidates are produced and decay in the vacuum region inside the beam pipe, well before the first layer of tracking, the Λ_c^+ acceptance is independent of a candidate's decay length.

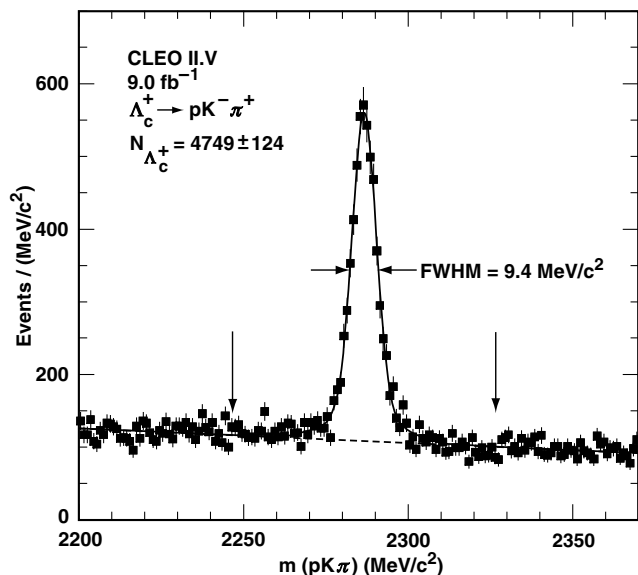


FIG. 1. Reconstructed mass distribution of Λ_c^+ candidates. The data (squares) are fit (solid line) to two Gaussians constrained to a single mean and a linear background (dotted line). There are $4749 \pm 124 \Lambda_c^+ \rightarrow pK^-\pi^+$ signal events. All events between the arrows ($\pm 40 \text{ MeV}/c^2$, or $\pm 11.1 \sigma_{\text{narrow}}$, of the Λ_c^+ signal peak) are used in the nominal unbinned maximum likelihood fit.

The Λ_c^+ lifetime is extracted from the proper time distribution with an unbinned maximum likelihood fit [11]. There are three inputs to the fit for each Λ_c^+ candidate: the measured proper time t_i , the estimated uncertainty of the measured proper time $\sigma_{t,i}$, and a reconstructed mass-dependent signal probability $p_{\text{sig},i}$. The signal probability distribution is obtained from a fit of the reconstructed mass distribution to two Gaussians constrained to the same mean for the signal and a linear function for the background. The likelihood function is

$$L(\tau_{\Lambda_c^+}, f_{\text{bg}}, \tau_{\text{bg}}, S, f_{\text{mis}}, \sigma_{\text{mis}}, f_{\text{wide}}) = \prod_i \int_0^\infty dt' \left[\underbrace{p_{\text{sig},i} E(t' | \tau_{\Lambda_c^+})}_{\text{signal fraction}} + \underbrace{(1 - p_{\text{sig},i}) [f_{\text{bg}} E(t' | \tau_{\text{bg}}) + (1 - f_{\text{bg}}) \delta(t')]}_{\text{background fraction}} \right] \\ \times \left[\underbrace{(1 - f_{\text{mis}} - f_{\text{wide}}) G(t_i - t' | S \sigma_{t,i})}_{\text{proper time resolution}} + \underbrace{f_{\text{mis}} G(t_i - t' | \sigma_{\text{mis}}) + f_{\text{wide}} G(t_i - t' | \sigma_{\text{wide}})}_{\text{mismeasured fraction}} \right],$$

where the product is over the Λ_c^+ candidates, $G(t | \sigma) \equiv \exp(-t^2/2\sigma^2)/\sqrt{2\pi}\sigma$, and $E(t | \tau) \equiv \exp(-t/\tau)/\tau$. The seven output parameters of the lifetime fit are $\tau_{\Lambda_c^+}$, f_{bg} , τ_{bg} , S , f_{mis} , σ_{mis} , and f_{wide} . The parameter $\tau_{\Lambda_c^+}$ is the Λ_c^+ lifetime. Each candidate is weighted in the fit according to its proper time uncertainty $\sigma_{t,i}$. The fit allows for a global scale factor S for the proper time uncertainty estimates. For a small fraction of candidates f_{mis} the fitted uncertainty $S\sigma_{t,i}$ underestimates the true uncertainty. Track

reconstruction errors such as those caused by hard multiple scattering are examples of such mismeasurements. The proper time distribution of the background is modeled by a fraction f_{bg} having a background lifetime τ_{bg} with the remaining background having zero lifetime. In order to estimate the background properties, we include the candidates in a wide region of $\pm 40 \text{ MeV}/c^2$ ($\pm 11.1 \sigma_{\text{narrow}}$) around the nominal Λ_c^+ mass in the unbinned maximum

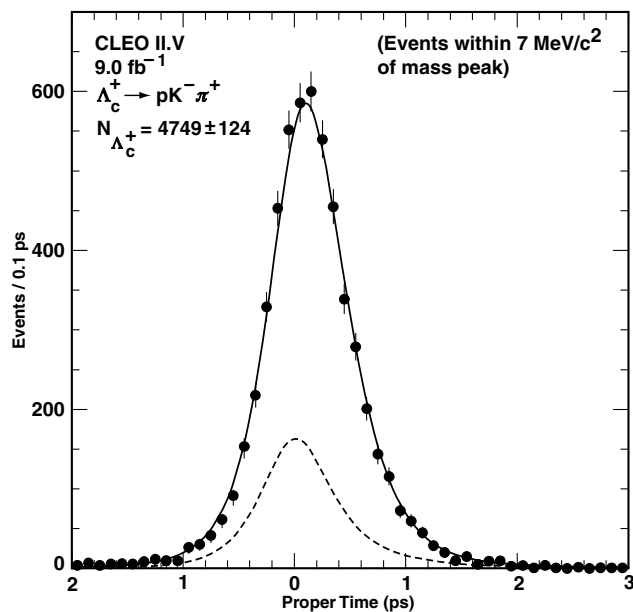


FIG. 2. Reconstructed proper time distribution (points) of Λ_c^+ candidates within $7 \text{ MeV}/c^2$ of the Λ_c^+ signal peak. Overlaid is a representation of the unbinned maximum likelihood lifetime fit scaled to the $\pm 7 \text{ MeV}/c^2$ reconstructed mass region (solid line). The fitted background component scaled to the $\pm 7 \text{ MeV}/c^2$ reconstructed mass region is also shown (dotted line).

likelihood fit. We account for mismeasured candidates with two Gaussians in the fit. In order to accommodate a small fraction f_{wide} of candidates that fall outside the resolution parameterization, a wide Gaussian ($\sigma_{\text{wide}} = 8 \text{ ps}$) is used to approximate a flat distribution. Figure 2 shows the proper time distribution of events within $7 \text{ MeV}/c^2$ of the Λ_c^+ signal peak and the results of the unbinned maximum likelihood fit scaled to the $\pm 7 \text{ MeV}/c^2$ reconstructed mass region. The fit converges to $\tau_{\Lambda_c^+} = (178.6 \pm 6.9) \text{ fs}$, where the uncertainty is statistical only. The fit also yields a global proper time uncertainty scale factor S of 1.1. The correlations between the Λ_c^+ lifetime and the other fit parameters range from -0.26 to 0.10 , and the $\chi^2/\text{d.o.f.}$ of the fit to the proper time distribution is $126/199$.

Consistency checks are performed by measuring the lifetime as functions of azimuthal angle, polar angle, momentum of the Λ_c^+ candidate, charge of the candidate, and data taking period. No statistically significant variation is found in any of these variables. The lifetime is also measured as a function of reconstructed mass in the background regions for CLEO data and simulated Monte Carlo events. The lifetimes are consistent with being uniform, and thus properly parametrized.

The contributions considered in the systematic uncertainty for the Λ_c^+ lifetime are listed in Table I and are described below. Decay vertex measurement errors lead to decay length errors which in turn could lead to an error in the lifetime measurement. A $(0.0 \pm 0.9) \mu\text{m}$ bias in the decay vertex position is estimated from a “zero-lifetime”

TABLE I. Contributions to the systematic uncertainty for the Λ_c^+ lifetime.

Contribution	Uncertainty (fs)
Decay vertex resolution	± 2.2
Global detector scale	± 0.1
Beam spot position	Negligible
Λ_c^+ mass measurement	± 0.05
Λ_c^+ momentum measurement	$^{+0.2}_{-0.1}$
Signal probability from mass fit	$^{+0.5}_{-0.7}$
$t - m(pK\pi)$ correlation	± 2.3
Large proper times	± 0.9
Statistics of Monte Carlo sample	± 2.8
Total	± 4.4

sample of $\gamma\gamma \rightarrow \pi^+\pi^-\pi^+\pi^-$ events. To obtain the corresponding proper time bias, the error of the decay vertex position bias is multiplied by the average $1/\gamma\beta c$ of the Λ_c^+ candidates. The vertices of events having interactions at the beam pipe are used to determine a relative radial position uncertainty of $\pm 0.2\%$. The quadrature sum of these uncertainties yields the systematic uncertainty due to the decay vertex measurement. The global detector scale is known to a precision of $\pm 0.1\%$ from detailed surveys using beam pipe interactions. A systematic uncertainty of $\pm 0.1 \text{ fs}$ is assigned. In order to determine the sensitivity of the analysis to the beam spot position, the vertical beam spot position is shifted $\pm 2 \mu\text{m}$, the uncertainty of the beam spot position, and the decay lengths of the Λ_c^+ candidates from CLEO data are recalculated. The differences between these shifted lifetimes and the nominal lifetime are included as a systematic uncertainty.

The uncertainty in the Λ_c^+ mass [2] and the Λ_c^+ momentum scale lead to systematic errors since these quantities are used in the conversion of decay lengths to proper times. The statistical uncertainty of the signal probability assigned to each Λ_c^+ candidate leads to systematic uncertainties in the fitted lifetimes, which are estimated by coherently varying the signal probability of each candidate by its statistical uncertainty and repeating the fits. There also exists a correlation between the measurements of the proper time t and the Λ_c^+ candidate reconstructed mass $m_{pK\pi}$. This correlation is measured in simulated events and confirmed in data to estimate a corresponding systematic uncertainty.

Poorly measured Λ_c^+ candidates are another source of systematic uncertainty. These candidates are accounted for in the unbinned maximum likelihood fit with a wide Gaussian that approximates a flat distribution ($\sigma_{\text{wide}} = 8 \text{ ps}$). Another method of accounting for candidates with large proper times is to omit the wide Gaussian component from the likelihood function and fit the candidates in a restricted proper time interval. The systematic uncertainty due to these candidates is estimated from the maximum variation of $\tau_{\Lambda_c^+}$ in varying the width of the wide Gaussian from 8 to 12 ps and removing the wide Gaussian in a restricted proper time fit ($|t| < 4 \text{ ps}$).

Other possible sources of lifetime measurement bias include Λ_c^+ selection requirements and parametrization of the background in the likelihood function. These are checked by performing the unbinned maximum likelihood fit on an artificial sample composed of background events extracted from e^+e^- annihilation data and simulated $\Lambda_c^+ \rightarrow pK^-\pi^+$ events with a known average lifetime of 206.2 fs. Accurately measuring the lifetime of this combined sample is an important test of the unbinned maximum likelihood method. The lifetime obtained from the maximum likelihood fit, (205.2 ± 2.8) fs, is consistent with the known input lifetime of the signal Monte Carlo sample. The statistical uncertainty of this measured lifetime, 2.8 fs, is included as a contribution to the total systematic uncertainty. The lifetime difference of -1.0 fs is subtracted from the lifetime extracted from data yielding a corrected Λ_c^+ lifetime of (179.6 ± 6.9) fs, where the uncertainty is statistical only. The total systematic uncertainty of 4.4 fs is obtained by adding the individual contributions in quadrature.

In summary, a new measurement of the Λ_c^+ lifetime using 9.0 fb^{-1} of integrated luminosity has been made with the CLEO II.V detector. The measured Λ_c^+ lifetime is $(179.6 \pm 6.9 \pm 4.4)$ fs, where the first uncertainty is statistical and the second systematic. This result is about 2σ lower than the PDG [2] world average Λ_c^+ lifetime of (206 ± 12) fs. This is the first Λ_c^+ lifetime measurement made in a nonfixed target environment.

We gratefully acknowledge the effort of the CESR staff in providing us with excellent luminosity and running conditions. This work was supported by the National Science Foundation, the U.S. Department of Energy, the Research Corporation, the Natural Sciences and Engineering Research Council of Canada, the A. P. Sloan

Foundation, the Swiss National Science Foundation, the Texas Advanced Research Program, and the Alexander von Humboldt Stiftung.

*Permanent address: University of Cincinnati, Cincinnati, OH 45221.

†Permanent address: Massachusetts Institute of Technology, Cambridge, MA 02139.

- [1] G. Bellini, I. Bigi, and P.J. Dornan, *Phys. Rep.* **289**, 1 (1997), and references contained within.
- [2] Particle Data Group, D.E. Groom *et al.*, *Eur. Phys. J. C* **15**, 1 (2000).
- [3] E687 Collaboration, P.L. Frabetti *et al.*, *Phys. Rev. Lett.* **71**, 827 (1993); *Phys. Lett. B* **323**, 459 (1994); E691 Collaboration, J.R. Raab *et al.*, *Phys. Rev. D* **37**, 2391 (1988); E791 Collaboration, E.M. Aitala *et al.*, *Phys. Lett. B* **445**, 449 (1999).
- [4] CLEO Collaboration, Y. Kubota *et al.*, *Nucl. Instrum. Methods Phys. Res., Sect. A* **320**, 66 (1992).
- [5] The inner radius of the beam pipe is 1.875 cm. The three layers of silicon are located at 2.35, 3.25, and 4.75 cm from the detector origin.
- [6] T. Hill, *Nucl. Instrum. Methods Phys. Res., Sect. A* **418**, 32 (1998).
- [7] P. Billoir, *Nucl. Instrum. Methods Phys. Res., Sect. A* **225**, 352 (1984).
- [8] We use a GEANT-based computer model to simulate the response of the CLEO detector. R. Brun *et al.*, GEANT 3.15, CERN Report No. DD/EE/84-1, 1987.
- [9] The right handed coordinate system has the z axis along the e^+ beam direction and the y axis upward.
- [10] D. Cinabro *et al.*, *Phys. Rev. E* **57**, 1193 (1998).
- [11] G. Bonvicini *et al.*, *Phys. Rev. Lett.* **82**, 4586 (1999).